

PAPER

## Effects of interlayer and bi-quadratic exchange coupling on layered triangular lattice antiferromagnets

To cite this article: M Li *et al* 2020 *J. Phys.: Condens. Matter* **32** 135803

View the [article online](#) for updates and enhancements.



**IOP | ebooks™**

Bringing you innovative digital publishing with leading voices to create your essential collection of books in STEM research.

Start exploring the [collection](#) - download the first chapter of every title for free.

# Effects of interlayer and bi-quadratic exchange coupling on layered triangular lattice antiferromagnets

M Li<sup>id</sup>, M L Plumer, and G Quirion

Department of Physics and Physical Oceanography, Memorial University, St. John's, Newfoundland A1B 3X7, Canada

E-mail: [ming.li@mun.ca](mailto:ming.li@mun.ca)

Received 23 July 2019, revised 10 November 2019

Accepted for publication 4 December 2019

Published 2 January 2020



## Abstract

The magnetic field evolution of ground spin states of the stacked planar triangular antiferromagnet with antiferromagnetic interlayer interaction  $J_c$  is explored using a minimal 3D classical Heisenberg model. A bi-quadratic coupling is also used to mimic the effect of spin fluctuations (Zhitomirsky 2015 *J. Phys.: Conf. Ser.* **592** 012110) which are known to stabilize the magnetization plateau. A single ion anisotropy is included and states with a magnetic field applied in the  $ab$  plane and along the  $c$  axis are determined. For  $\mathbf{H} \parallel ab$ -plane, an additional new state, in contrast to 2D model (Zhitomirsky 2015 *J. Phys.: Conf. Ser.* **592** 012110), is obtained with weak interlayer interaction, while the magnetization plateau vanishes at large  $J_c$  and other new states with  $z$  components of spins emerge. For  $\mathbf{H} \parallel c$ -axis, an extra state, compared with 2D model, is obtained with a weak interlayer interaction. When  $J_c$  is large enough, only the state corresponding to the Umbrella phase in 2D model exits.

Keywords: frustrated antiferromagnet, stacked triangular lattice, interlayer interaction

(Some figures may appear in colour only in the online journal)

## 1. Introduction

The two-dimensional (2D) geometrically frustrated triangular lattice antiferromagnets (TLAFs) have been widely studied in a variety of compounds over recent decades. These systems are known to display various exotic magnetic states due to the extensive degeneracy associated with magnetic frustration on a triangular lattice [2–4]. In particular, one of these exotic states, associated with a collinear up–up–down (uud) state, leads to the observation of a magnetization plateau in many quasi-2D TLAFs with easy-plane anisotropy at a value of  $1/3$  of the magnetization saturation ( $M_s$ ) [5–16]. This plateau in the magnetization is believed to be stabilized by thermal/quantum spin fluctuations [1, 17–21]. This conclusion is well supported by 2D quantum numerical studies [1, 17–20] and Monte Carlo simulation [21, 22] which successfully reproduce the observed phase sequence ( $120^\circ$  state at zero field, Y state at low field, uud state at intermediate field, and V state at high field) for a magnetic field applied in the basal plane. However,

a new phase between the uud state and the V state was recently proposed by Yamamoto *et al* [23, 24] who took into consideration the interlayer exchange coupling. This finding could account for the magnetization anomaly observed near  $3/5 M_s$  in  $\text{Ba}_3\text{CoSb}_2\text{O}_9$  with  $\mathbf{H} \parallel ab$ -plane [10], and it indicates the importance of the interlayer interaction, even when it is weak compared to the intralayer interaction. So far, the effect of the interlayer interaction in TLAFs has been limited to a few studies [23, 24], hence there is still a need to explore how the magnetic properties evolve as a function of the interlayer exchange coupling.

In this work, the effect of the antiferromagnetic interlayer interaction on the ground states of the layered easy-plane TLAFs is explored using a 3D classical Heisenberg model with bi-quadratic exchange coupling ( $\gamma$ ) between nearest-neighbour ions within the basal plane. The bi-quadratic coupling ( $\gamma$ ) plays an important role as it mimics the effect of spin fluctuations [1, 25] which are known to stabilize the magnetization plateau (uud state). On the other hand, the microscopic

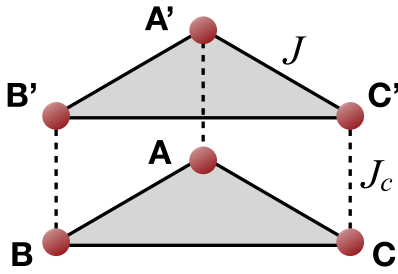


**Figure 1.** Two-layer triangular lattice with intralayer interaction  $J$  and interlayer interaction  $J_c$ .

origin of the biquadratic exchange coupling term can also be associated with the spin-lattice coupling (magnetoelastic coupling) [26–28]. The single ion anisotropy ( $D$ ) is also considered and the magnetic states with  $\mathbf{H} \parallel a$ -axis and  $c$ -axis are determined and compared with existing experimental magnetic phase diagrams.

Without the interlayer interaction ( $J_c = 0$ ), the model accounts for the  $120^\circ$  state, Y state, uud state, and V state with  $\mathbf{H} \parallel a$ -axis as obtained from 2D Monte Carlo simulations [21]. Our minimal classical model allows us to study in detail how the magnetic properties of TLAFs, with easy-plane anisotropy ( $D = 0.05$ ) and bi-quadratic coupling ( $\gamma = -0.05$ ), evolve as a function of the interlayer coupling parameter ( $J_c$ ). Moreover, consistent with [24] and in contrast to the 2D model [1], a new state between the uud and the V phase is observed for weak interlayer interaction. The results also show that the width of the magnetization plateau decreases as  $J_c$  increases, and vanishes at  $J_c \sim 0.1$ . Within a small interlayer coupling range ( $0.15 < J_c < 0.16$ ), two new states with a small alternating  $z$ -component of spins emerge. For  $\mathbf{H} \parallel c$ -axis, the Umbrella (U) state and  $V_z$  state, observed in experiments [10–12], are reproduced without the interlayer interaction ( $J_c = 0$ ), while a state between the U and  $V_z$  states is obtained with weak interlayer interaction and disappears at a medium value of  $J_c$  ( $\sim 0.06$ ). When  $J_c$  is large ( $> 0.2$ ), only the state corresponding to the Umbrella phase exits.

The remainder of this paper is organized as follows. We first describe the 3D Heisenberg model representing a two-layer triangular lattice in section 2. The magnetization obtained for that effective model, along with the spin configurations associated with the different magnetic orders, are shown in sections 3 and 4. For  $\mathbf{H} \parallel ab$ -plane, the results with  $0 \leq J_c \leq 0.21$  are presented in section 3, while the results for  $\mathbf{H} \parallel c$ -axis with  $0 \leq J_c \leq 0.24$  are presented in section 4. Finally, summary and discussion are presented in section 5.

## 2. Model: two-layer triangular lattice

The two-layer equilateral triangular lattice system is shown in figure 1, where each magnetic layer is comprised of three sublattices with spins at triangle vertices. In this model, equation (1) represents the energy per plane where only the intralayer exchange coupling constant ( $J$ ) between the nearest neighbouring (NN) spins is taken into consideration. The Heisenberg Hamiltonian per layer can be written as

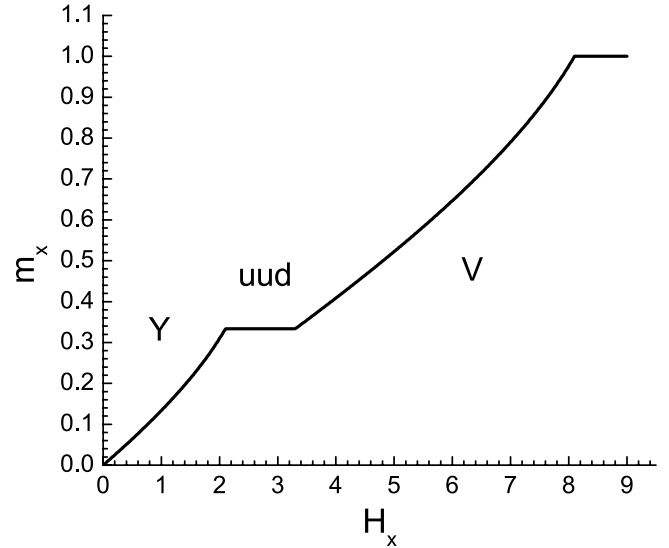


**Figure 2.** Magnetization process of the single-layer TLAFs with  $\gamma = -0.05$ ,  $D = 0.05$ , and  $\mathbf{H} \parallel x$ -axis.

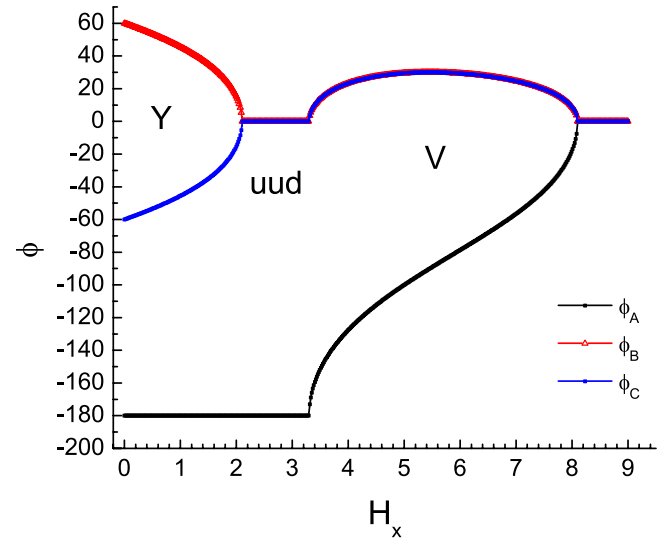


**Figure 3.** The field dependence of the angles  $\phi_i$  for the single-layer TLAFs with  $\gamma = -0.05$ ,  $D = 0.05$ , and  $\mathbf{H} \parallel x$ -axis. The angles  $\theta_i = 90^\circ$  due to the easy-plane anisotropy.

$$E_\alpha = J \sum_{i \neq j} \mathbf{S}_{i\alpha} \cdot \mathbf{S}_{j\alpha} - \frac{1}{3} \mathbf{H} \cdot \sum_i \mathbf{S}_{i\alpha} + \gamma \sum_{i \neq j} (\mathbf{S}_{i\alpha} \cdot \mathbf{S}_{j\alpha})^2 + D \sum_i S_{i\alpha_z}^2, \quad (1)$$

where  $E_\alpha$  denotes the energy of layer  $\alpha$  (stacked along the  $c$ -axis),  $i$  denotes one of the three magnetic ions at a triangle vertex. The first term corresponds to the intralayer coupling energy ( $J$ ), the second term is Zeeman energy, the third term is the bi-quadratic coupling energy ( $\gamma$ ) which stabilizes the magnetization plateau, and the last term is the single ion anisotropy energy ( $D$ ). Furthermore, taking into consideration only the interlayer nearest neighbouring exchange coupling ( $J_c$ ), two layers are sufficient for describing ground states of the

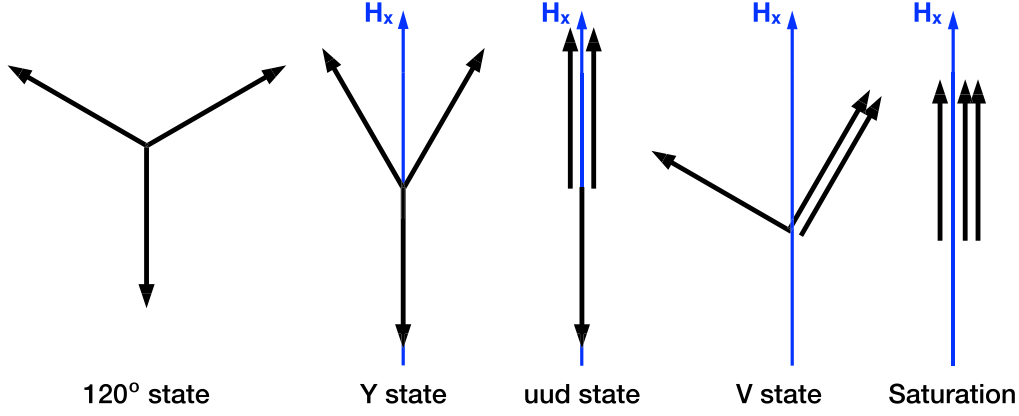


**Figure 4.** Spin configurations of a 2D TLAFs with easy-plane anisotropy and  $\mathbf{H} \parallel x$ -axis in different phases. Arrows represent spins of the ions on the sublattice vertices. Also see [24].

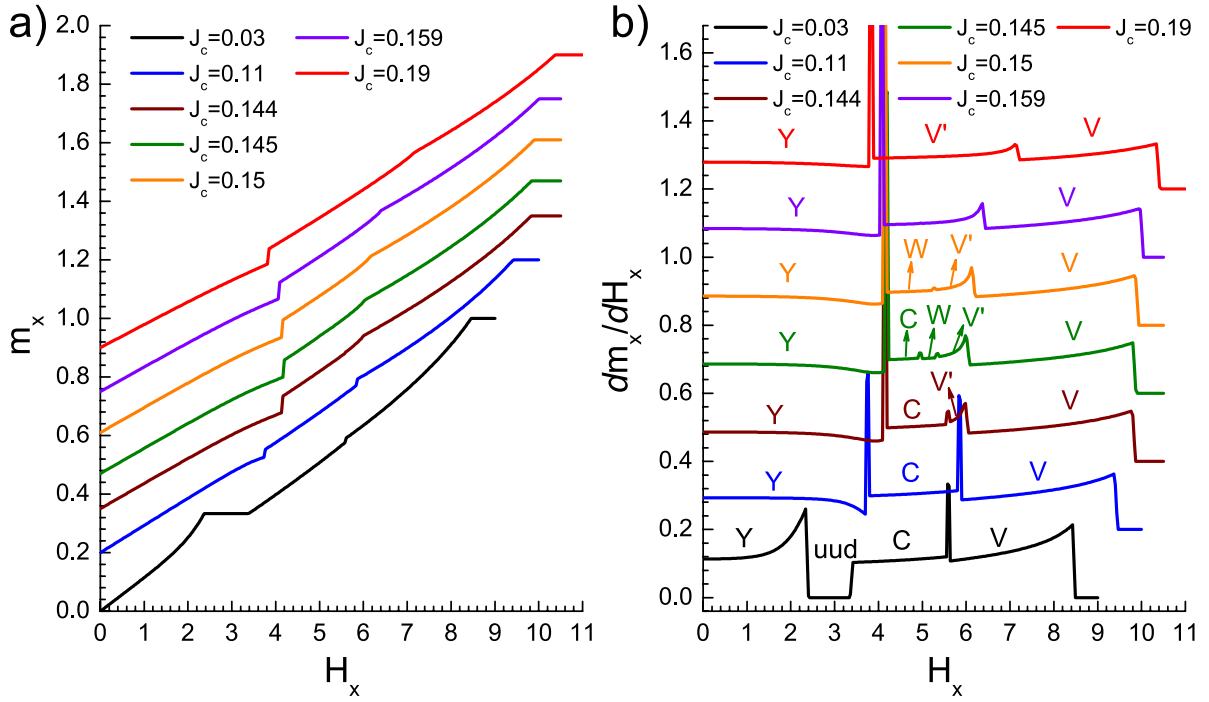


**Figure 5.** (a) Magnetization process of the two-layer TLAFs with  $\gamma = -0.05$ ,  $D = 0.05$ , and  $\mathbf{H} \parallel x$ -axis. (b) The first derivatives of the magnetizations assisting to identify phase transitions. The curves are shifted vertically for clarity.

system [24]. The total Hamiltonian for two layers (6 spins) can be written as

$$E = \frac{1}{2} \sum_{\alpha} E_{\alpha} + J_c \sum_{\alpha \neq \beta} \sum_i \mathbf{S}_{i\alpha} \cdot \mathbf{S}_{i\beta}, \quad (2)$$

where the second term is the sum over the interlayer nearest neighbouring spins. We omit the interlayer bi-quadratic coupling, since it is expected much smaller than  $\gamma$  and does not affect the results due to the absence of frustration between two layers [29]. The magnetization per site is given by

$$\mathbf{m} = \frac{1}{6} \sum_{\alpha} \sum_i \mathbf{S}_{i\alpha}. \quad (3)$$

Here the spins are written as 3D vectors described by the angles  $\phi_{i\alpha}$  and  $\theta_{i\alpha}$ :

$$\mathbf{S}_{i\alpha} = (\cos \phi_{i\alpha} \sin \theta_{i\alpha}, \sin \phi_{i\alpha} \sin \theta_{i\alpha}, \cos \theta_{i\alpha}). \quad (4)$$

Note that six spins are sufficient to capture ground state spin configurations in the present model with NN exchange only, as has been demonstrated previously [30, 31]. Minimizing the Hamiltonian (equation (2)) relative to  $\phi_{i\alpha}$  and  $\theta_{i\alpha}$  using the Nelder–Mead method [32], the magnetization and the spin configurations are obtained for different parameter and field values.

In this work, the coefficient of the antiferromagnetic intra-layer exchange coupling is set to  $J = 1$ , while the effect of the antiferromagnetic interlayer coupling ( $0 < J_c < 0.24$ ) is explored. In order to account for the collinear spin configuration (uud state), the bi-quadratic coupling coefficient  $\gamma$  must be negative [1]. Here  $\gamma$  is set to  $-0.05$  in order to obtain a magnetization plateau width consistent with some

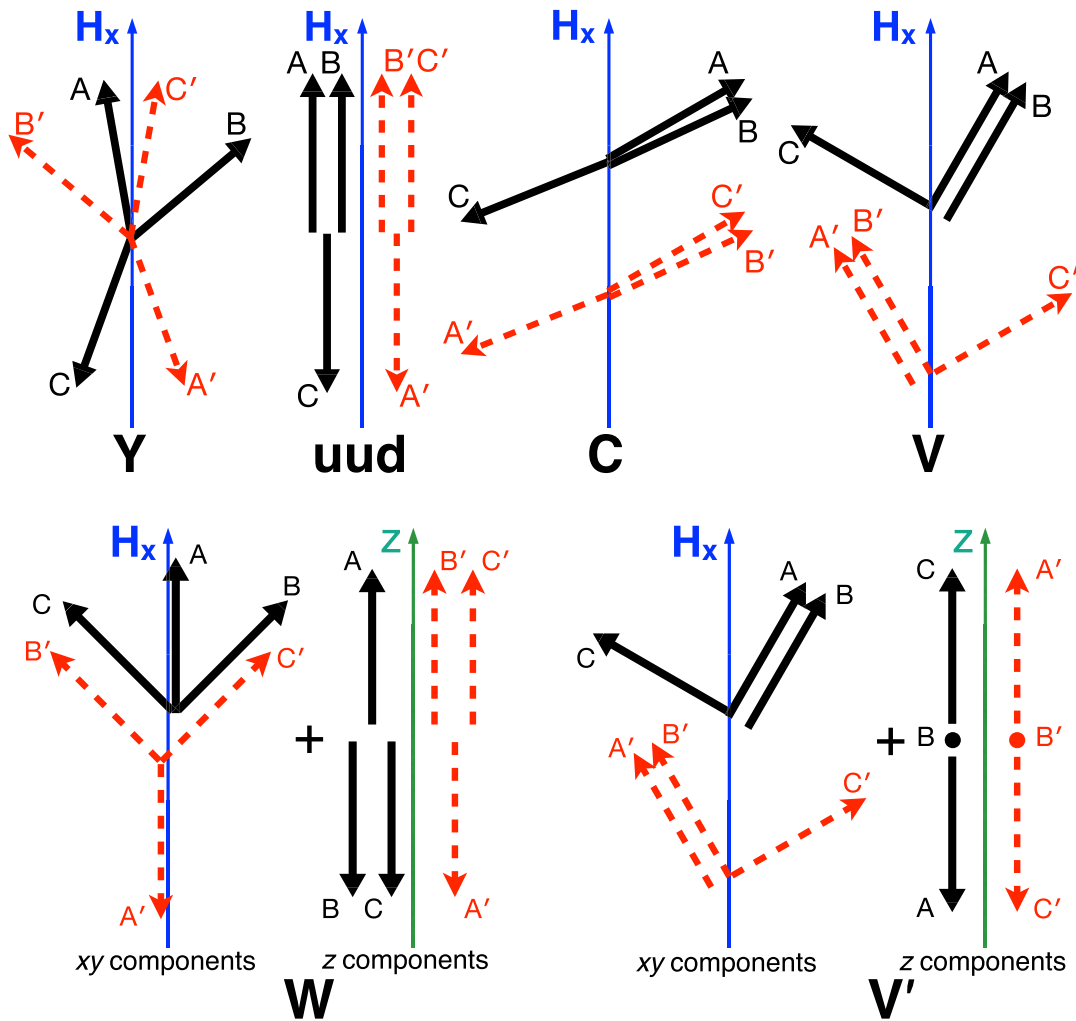


**Figure 6.** Spin configurations of TLAFs with interlayer interaction and  $\mathbf{H} \parallel x$ -axis in different phases. Black solid arrows (A, B, C) and red dotted arrows ( $A'$ ,  $B'$ ,  $C'$ ) represent spins at the sublattice vertices in different layers, respectively. (See figure 1) The Y, uud, C and V states for two layers have been shown in [24] with weak interlayer interaction, while W and  $V'$  are new states obtained with larger  $J_c$ .

experimental results [10, 11]. Since the single ion anisotropy and the exchange anisotropy have the same effect in the case of easy-plane anisotropy with the field in the plane [33], we set  $D = 0.05$  close to the experimental value of the exchange anisotropy as determined for  $\text{Ba}_3\text{CoSb}_2\text{O}_9$  [10].

### 3. $\mathbf{H} \parallel ab$ -plane

We first present results obtained using the effective Hamiltonian equation (2) by setting  $J_c = 0$  with  $\mathbf{H} \parallel x$ -axis where the  $x$ -axis is in the  $ab$ -plane. The magnetization curve  $m_x$  and the field dependence of the angles  $\phi_i$  are shown in figures 2 and 3, respectively, while the different spin configurations are presented in figure 4. For  $H = 0$ , the ground state corresponds to the  $120^\circ$  spin structure. The so-called Y state is stabilized at low fields, the magnetization plateau associated with the uud state follows and then the V state before the magnetization saturation is obtained at high fields. The results presented in figures 2 and 4, obtained using the classical 2D

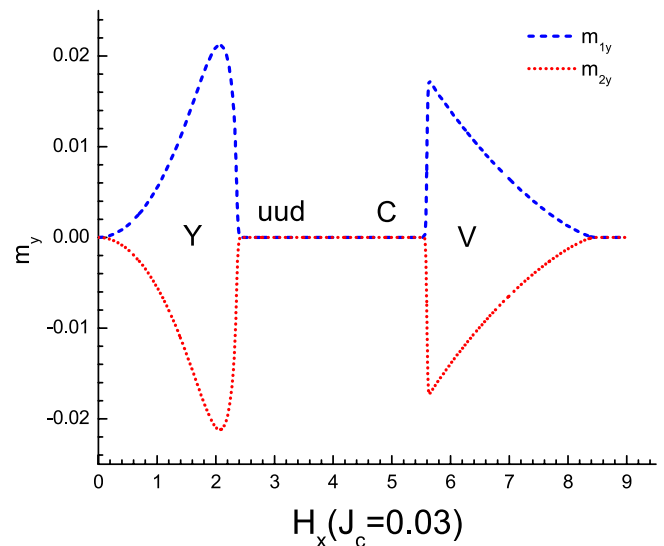


**Figure 7.** The  $y$ -component magnetization in each layer with  $J_c = 0.03$ ,  $\gamma = -0.05$ , and  $D = 0.05$ .

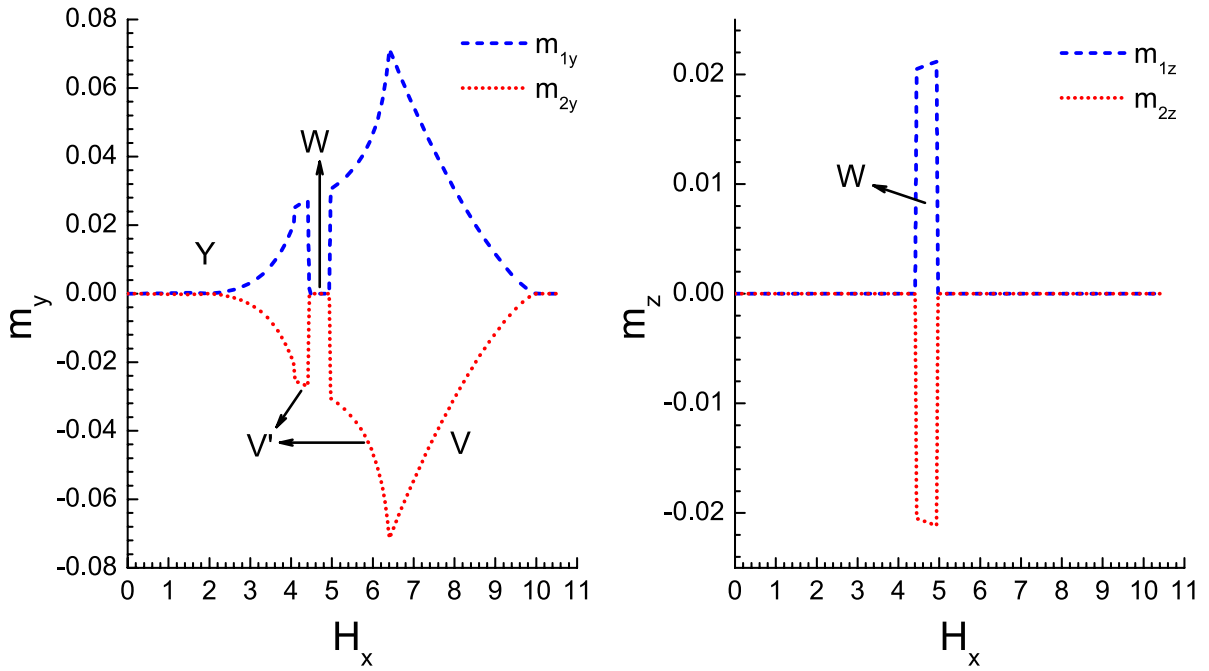


**Figure 8.** The  $y$  (left) and  $z$  (right) components of the magnetization in each layer with  $J_c = 0.159$ ,  $\gamma = -0.05$ , and  $D = 0.05$  are presented for different phases.

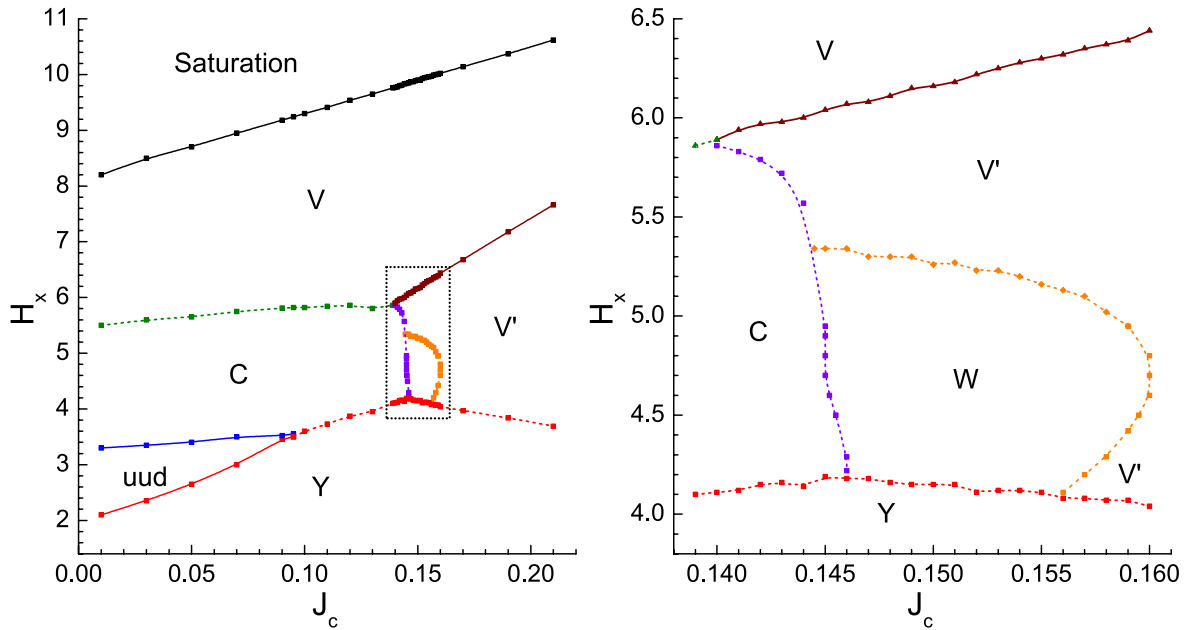


**Figure 9.** Left:  $H_x$ - $J_c$  diagram of two-layer TLAFs with  $\gamma = -0.05$ ,  $D = 0.05$ . Phases are described in figure 6. Right: the enlarged region indicated by the dotted rectangle in the left diagram. The dashed and solid lines indicate first and second order phase transitions, respectively.

effective Hamiltonian equation (1) are in good agreement with previous results based on 2D Monte Carlo simulations [21] and 2D quantum models [1, 17–20, 23, 24]. Considering that the effective Hamiltonian (equation (1)) adequately describes the magnetic properties of 2D TLAF, it can be easily modified (equation (2)) in order to explore the properties of 3D TLAF with easy-plane anisotropy.

In figure 5(a), we present the magnetization curves  $m_x$  for different values of the antiferromagnetic interlayer coupling coefficient  $J_c$  while figure 5(b) shows the derivatives of the

magnetizations in order to identify the critical fields. The spin configurations of the different states are shown in figure 6.

In the range  $0 < J_c < 0.1$ , compared with the 2D model magnetization (figure 2), one additional C (canted) phase is obtained between the plateau and the V phase, consistent with results published in [24]. The spin configurations for the quasi-2D Y state, uud state, C state and V state are sketched in figure 6. Furthermore, as shown in figure 7, the Y and V phases have a small none-zero  $y$ -component (perpendicular to the  $x$ -axis) of the magnetization which alternates from one

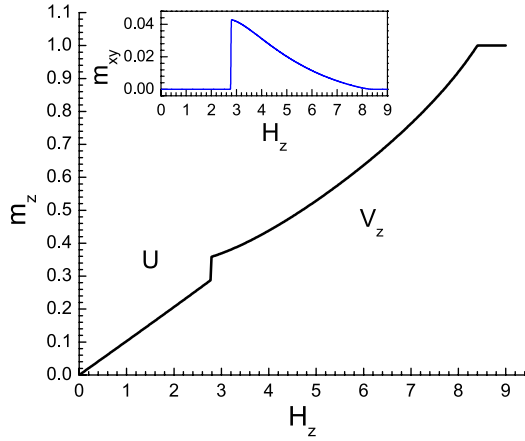


**Figure 10.** Magnetization process of the single-layer TLAFs with  $\gamma = -0.05$ ,  $D = 0.05$ , and  $\mathbf{H} \parallel z$ -axis. The inset shows the  $xy$  component of the magnetization.

plane to the next. This figure also clearly illustrates the first order character of the phase transition between the C and V states. Consequently, we conclude that interlayer interaction, even weak compared with the intralayer exchange interaction, stabilizes a new state and modifies the spin configurations relative to the 2D system.

For  $J_c$  larger than 0.1, as shown in figure 5(a), the magnetization plateau disappears. Therefore, in the range  $0.1 < J_c < 0.14$ , the system transforms directly from the Y state to the C state via a first-order transition indicated by a jump on the magnetization in figure 5(a).

For  $0.14 < J_c < 0.16$ , two new states, W state and  $V_l$ , are obtained whose spin configurations are presented in figure 6. In the W state, each layer develops a small  $z$ -component of the magnetization which alternates from one layer to the next (see figure 8), while the configuration in the  $xy$ -plane forms a W shape and a Y shape in different layers, respectively. In the  $V_l$  state, while the spin configuration in the  $xy$ -plane is identical to that of the the V phase, two spins in each layer have a small  $z$ -component in opposite directions, maintaining the  $z$ -component magnetization per plane to zero. Furthermore, the derivative of the magnetization (figure 5(b)) shows that  $Y \rightarrow V_l$ ,  $Y \rightarrow W$ ,  $Y \rightarrow C$ , and  $C \rightarrow V$  correspond to first order phase transitions.

To explain the appearance a spin polarization normal to the  $ab$ -plane in W and  $V_l$  states, we compare the energy of the anisotropic term ( $E_a$ ) and the interlayer interaction ( $E_c$ ), which involve the  $z$  component of the spins (see equation (5)).

$$E_a = \frac{D}{2} (S_{A_z}^2 + S_{A'_z}^2 + S_{B_z}^2 + S_{B'_z}^2 + S_{C_z}^2 + S_{C'_z}^2)$$

$$E_c = J_c (S_{A_z} S_{A'_z} + S_{B_z} S_{B'_z} + S_{C_z} S_{C'_z}). \quad (5)$$

When  $J_c$  is zero or very small, the energy is minimized by having no  $z$  component. However, when  $J_c$  is large enough ( $\sim 0.14$ ), the lowest energy can be reduced by having anti-parallel  $z$  component nearest neighbour interlayer spins.

We present in figure 9 the  $H_x$ - $J_c$  phase diagram for the two-layer TLAFs. The dashed and solid lines indicate first and second order phase transitions, respectively. As shown,

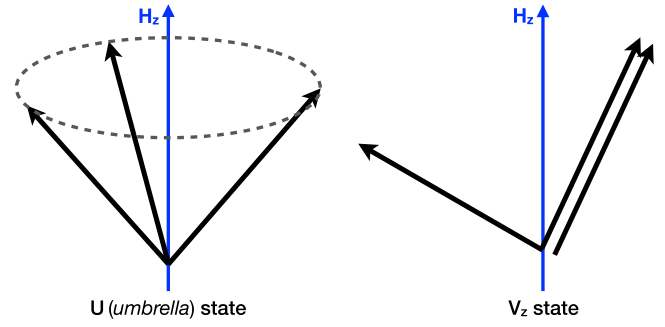


**Figure 11.** Spin configurations of a 2D TLAFs with easy-plane anisotropy and  $\mathbf{H} \parallel z$ -axis in different phases. Arrows represent spins of the ions on the sublattice vertices.

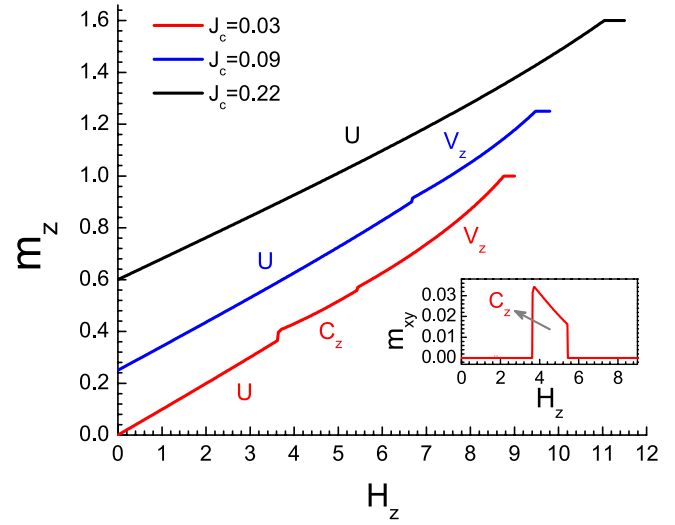


**Figure 12.** Left: magnetization process of the two-layer TLAFs with  $\gamma = -0.05$ ,  $D = 0.05$ , and  $\mathbf{H} \parallel z$ -axis. Right: the first derivatives of the magnetizations assisting to identify phase transitions. The curves are shifted vertically for clarity. The inset shows the  $xy$  component of the magnetization with  $J_c = 0.03$ .

the range of the magnetization plateau (uud state) decreases with increasing interlayer interaction and vanishes at  $J_c = 0.1$ . The C state is only obtained with a weak interlayer interaction and disappears at  $J_c = 0.146$ . When  $0.14 < J_c < 0.16$ , the W and  $V_l$  states, which have a spin  $z$  component, are stabilized. For  $J_c > 0.16$ , only the  $V_l$  state exists between the Y and V states. Therefore, we can conclude that the interlayer interaction plays an important role in the magnetization process of easy-plane TLAFs.

#### 4. $\mathbf{H} \parallel c$ -axis

With  $\mathbf{H} \parallel z \parallel \hat{c}$ , the magnetization curve  $m_z$  obtained from the one-layer model ( $J_c = 0$ ) is shown in figure 10, while the different spin configurations are presented in figure 11. The Umbrella state (U state) and  $V_z$  state, associated with the observation of a first order phase transition in experiments [10–12], are stabilized at low fields and high fields, respectively. Furthermore, the  $V_z$  state is also characterized by a small none-zero magnetization perpendicular to the  $z$ -axis (shown in the inset of figure 10).

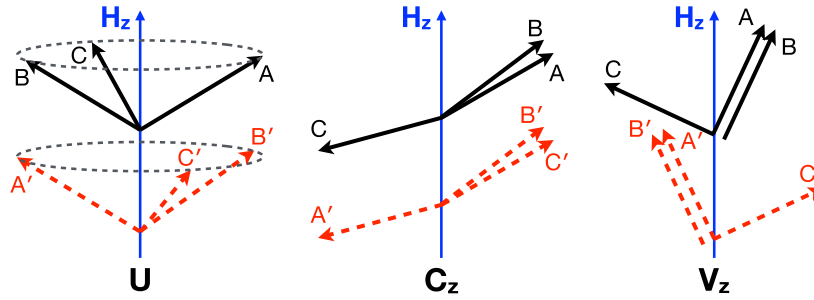


**Figure 13.** Spin configurations of TLAFs with the interlayer interaction and  $\mathbf{H} \parallel z$ -axis in different phases. Black solid arrows (A, B, C) and red dotted arrows ( $A'$ ,  $B'$ ,  $C'$ ) represent spins at the sublattice vertices in different layers, respectively.

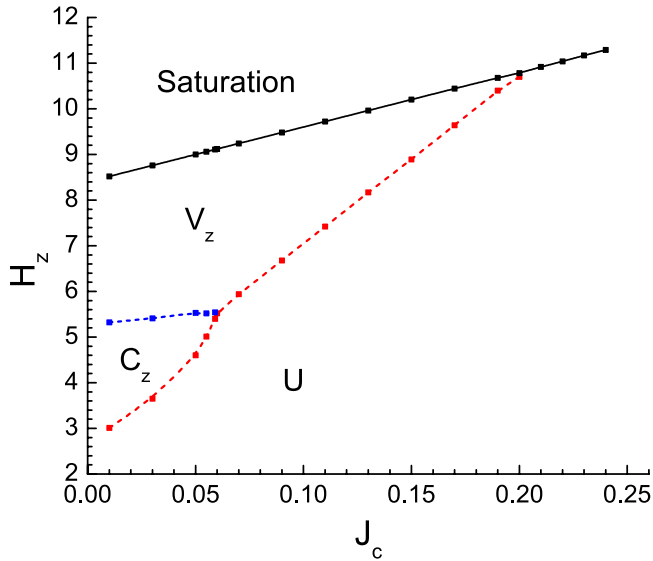


**Figure 14.**  $H_z$ - $J_c$  diagram of two-layer TLAFs with  $\gamma = -0.05$ ,  $D = 0.05$ . Phases are described in figure 13. The dashed and solid lines indicate first and second order phase transitions, respectively.

In figure 12, we present magnetization curves  $m_z$  for different values of the antiferromagnetic interlayer coupling coefficient  $J_c$ . For a weak interlayer interaction ( $0 < J_c < 0.06$ ), compared with the 2D model magnetization (figure 10), one extra  $C_z$  (canted) state is obtained between the U state and the  $V_z$  state. The spin configurations for the quasi-2D U state,  $V_z$  state and  $C_z$  state are sketched in figure 13. Different from the 2D model, the two-layer  $V_z$  state has no net  $xy$ -component magnetization perpendicular to the  $z$ -axis, while the  $C_z$  state has a small transverse magnetization as shown in the inset of figure 12. In the range  $0.06 < J_c < 0.2$ , U and  $V_z$  states are obtained and represented by the blue lines in figure 12. For  $J_c > 0.2$ , only the U state exists before the magnetization saturation, indicated by the black lines. The resulting  $H_z$ - $J_c$  phase diagram for the two-layer TLAFs is presented in figure 14 with dashed and solid lines representing first and second order phase transitions, respectively.

## 5. Summary and discussion

The ground state magnetization processes of TLAFs are calculated for both  $\mathbf{H}$  in the  $ab$ -plane and  $\mathbf{H} \parallel c$ -axis using a two-layer classical Heisenberg model with the single ion

anisotropy ( $D$ ) and the bi-quadratic exchange coupling ( $\gamma$ ). To study realistic 3D TLAFs, we explored the effect of the antiferromagnetic interlayer interaction ( $J_c$ ). Results with  $\mathbf{H} \parallel ab$ -plane and  $\mathbf{H} \parallel c$ -axis shows that the interlayer interaction plays a role for stabilizing the additional state (C state), consistent with [24]. This additional state could account for the magnetization anomaly observed near  $3/5 M_s$  in  $\text{Ba}_3\text{CoSb}_2\text{O}_9$  with  $\mathbf{H}$  in the  $ab$ -plane [10]. Other new states, not previously reported, are also observed with higher values of the interlayer interaction. The range of field, over which all states are stabilized, depends on the value of  $J_c$ . Moreover, the spin configurations of the W and  $V'$  states show the appearance of small  $z$  components due to the interlayer interaction competing with the single ion anisotropy. Due to this competition, the system exhibits complex magnetization processes, especially when  $0.144 < J_c < 0.146$  (see figure 9). It should be noticed that the values of  $J_c$  for obtaining the W and  $V'$ s states are large compared with the small  $J_c$  with which the magnetization plateau survives, but still about one order of magnitude smaller than the intralayer interaction  $J$ . Therefore, this model can still be considered to be quasi-2D, with the interlayer exchange coupling playing an important role. Furthermore, all ground states of the two layer model have the same ordering wave vector  $\mathbf{Q} = (1/3, 1/3, 1/2)$ . Future work using Monte Carlo simulation to explore the  $H$ - $T$  phase diagram, such as that on pyrochlore [28], would be of interest. We believe that a detailed analysis of relevant experimental results on existing and yet to be discovered TLAFs may benefit from the results present here.

## Acknowledgments

The authors wish to acknowledge the financial support of the Natural Sciences and Engineering Research Council of Canada (NSERC).

## ORCID iDs

M Li  <https://orcid.org/0000-0003-4239-6886>

## References

- [1] Zhitomirsky M E 2015 *J. Phys.: Conf. Ser.* **592** 012110

- [2] Collins M F and Petrenko O A 1997 *Can. J. Phys.* **75** 605
- [3] Balents L 2010 *Nature* **464** 199
- [4] Wosnitza J, Zvyagin S A and Zherlitsyn S 2016 *Rep. Prog. Phys.* **79** 074504
- [5] Ono T et al 2004 *J. Phys.: Condens. Matter* **16** S773
- [6] Fujii Y, Nakamura T, Kikuchi H, Chiba M, Goto T, Matsubara S, Kodama K and Takigawa M 2004 *Physica B* **346–7** 45 (*Proc. of the 7th Int. Symp. on Research in High Magnetic Fields*)
- [7] Ono T, Tanaka H, Aruga Katori H, Ishikawa F, Mitamura H and Goto T 2003 *Phys. Rev. B* **67** 104431
- [8] Tsujii H, Rotundu C R, Ono T, Tanaka H, Andracka B, Ingersent K and Takano Y 2007 *Phys. Rev. B* **76** 060406
- [9] Fortune N A, Hannahs S T, Yoshida Y, Sherline T E, Ono T, Tanaka H and Takano Y 2009 *Phys. Rev. Lett.* **102** 257201
- [10] Susuki T, Kurita N, Tanaka T, Nojiri H, Matsuo A, Kindo K and Tanaka H 2013 *Phys. Rev. Lett.* **110** 267201
- [11] Quirion G, Lapointe-Major M, Poirier M, Quilliam J A, Dun Z L and Zhou H D 2015 *Phys. Rev. B* **92** 014414
- [12] Sera A, Kousaka Y, Akimitsu J, Sera M, Kawamata T, Koike Y and Inoue K 2016 *Phys. Rev. B* **94** 214408
- [13] Ma J, Kamiya Y, Hong T, Cao H B, Ehlers G, Tian W, Batista C D, Dun Z L, Zhou H D and Matsuda M 2016 *Phys. Rev. Lett.* **116** 087201
- [14] Svistov L E, Smirnov A I, Prozorova L A, Petrenko O A, Demianets L N and Shapiro A Y 2003 *Phys. Rev. B* **67** 094434
- [15] White J S, Niedermayer C, Gasparovic G, Broholm C, Park J M S, Shapiro A Y, Demianets L A and Kenzelmann M 2013 *Phys. Rev. B* **88** 060409
- [16] Mitamura H et al 2014 *Phys. Rev. Lett.* **113** 147202
- [17] Honecker A, Schulenburg J and Richter J 2004 *J. Phys.: Condens. Matter* **16** S749
- [18] Sakai T and Nakano H 2011 *Phys. Rev. B* **83** 100405
- [19] Yoshikawa S-I, Okunishi K, Senda M and Miyashita S 2004 *J. Phys. Soc. Japan* **73** 1798
- [20] Götze O, Richter J, Zinke R and Farnell D 2016 *J. Magn. Magn. Mater.* **397** 333
- [21] Gvozdkova M V, Melchy P-E and Zhitomirsky M E 2011 *J. Phys.: Condens. Matter* **23** 164209
- [22] Lee D H, Joannopoulos J D, Negele J W and Landau D P 1986 *Phys. Rev. B* **33** 450
- [23] Yamamoto D, Marmorini G and Danshita I 2015 *Phys. Rev. Lett.* **114** 027201
- [24] Yamamoto D, Marmorini G and Danshita I 2016 *J. Phys. Soc. Japan* **85** 024706
- [25] Heinilä M T and Oja A S 1993 *Phys. Rev. B* **48** 7227
- [26] Wang F and Vishwanath A 2008 *Phys. Rev. Lett.* **100** 077201
- [27] Bergman D, Shindou R, Fiete G A and Balents L 2006 *Phys. Rev. B* **74** 134409
- [28] Penc K, Shannon N and Shiba H 2004 *Phys. Rev. Lett.* **93** 197203
- [29] Zhitomirsky M E 2019 private communication
- [30] Oyedele J A and Collins M F 1978 *Can. J. Phys.* **56** 1482–7
- [31] Kawamura H 1984 *J. Phys. Soc. Japan* **53** 2452–5
- [32] Nelder J A and Mead R 1965 *Comput. J.* **7** 308–13
- [33] Miyashita S 1986 *J. Phys. Soc. Japan* **55** 3605